

# Automated Classification of Airborne Laser Scanning Point Clouds

Christoph Waldhauser      Ronald Hochreiter  
Johannes Otepka      Norbert Pfeifer      Sajid Ghuffar  
Karolina Korzeniowska      Gerald Wagner

April 2014

## Abstract

Making sense of the physical world has always been at the core of mapping. Up until recently, this has always dependent on using the human eye. Using airborne lasers, it has become possible to quickly “see” more of the world in many more dimensions. The resulting enormous point clouds serve as data sources for applications far beyond the original mapping purposes ranging from flooding protection and forestry to threat mitigation. In order to process these large quantities of data, novel methods are required. In this contribution, we develop models to automatically classify ground cover and soil types. Using the logic of machine learning, we critically review the advantages of supervised and unsupervised methods. Focusing on decision trees, we improve accuracy by including beam vector components and using a genetic algorithm. We find that our approach delivers consistently high quality classifications, surpassing classical methods.

## 1 Introduction

Surveying the very planet we live on has been an ongoing effort since the dawn of mankind. From the early maps of Anatolia to modern geospatial intelligence, the mission of any map was always to make sense of the world around us. Boosting map drawing with the latest advances of machine learning has the potential to largely facilitate the generation of maps and extend their usefulness into application domains beyond path finding.

In this chapter, we present the combined efforts of academia and industry to create a framework for the automated generation of maps. The basis for this project is airborne laser scanning: the systematic recording and digitizing of ground by means of laser emitted from aircraft. The resulting point clouds of the environment are then automatically classified into ground cover types, using supervised learning and evolutionary computation approaches.

This chapter is organized as follows. In a first section we describe the technical background of airborne laser scanning. Section 3 details the work related to develop automated classification models. There we will compare the practical aspects of supervised and unsupervised approaches as well as detail the supervised classification approach we implemented and evolutionary computation extensions to it. That section also features a description of the data set we used to empirically test our approaches. The aspects of implementing our model in industry applications is discussed in the subsequent section 4. We close with some concluding remarks pointing to future research.

## 2 Airborne Laser Scanning Point Clouds

### 2.1 Measurement principle

Airborne Laser Scanning (ALS) is a remote sensing method for obtaining geometrical and additional information about objects not in contact with the sensor, i.e. the laser scanner. A laser scanner emits a short pulse of infrared light which travels through the atmosphere and is scattered and partially absorbed by any objects in the instantaneous field of view of the laser beam. If diffuse reflection occurs, which is the standard case for many object surfaces, including, e.g., vegetation, bare ground, and building surfaces, a portion of the incident light is scattered back to the sensor. There, the backscattered signal is detected and recorded. The time lag between emission of the pulse and detection of its echo is the two way travel time from the sensor to the object. With the known speed of light this time lag is turned into the distance from sensor to object. This is also called laser range finding (LRF). In laser scanning, the beam is scanned across the entire field of view, thus covering a larger extent. Rotating mirrors and comparable devices are used to deflect the laser beam and cover large areas. With the known orientation of the mirror and the known position of the laser scanner in a global Earth fixed coordinate system (e.g. WGS84, in UTM projection), the location of the objects at which the laser pulse was scattered can be computed. This provides a so-called 3D point cloud: a set of points, each with 3 co-ordinates  $x, y, z$ . These points are obtained in the sensor co-ordinate system.

In airborne laser scanning the scanner is mounted on a flying platform (fixed wing or helicopter). Its position is measured with Global Navigation Satellite Systems (GNSS, e.g., GPS). The angular attitude of the sensor platform inside the aircraft is observed with Inertial Measurement Unit (IMU, comprised of accelerometers and gyros). The laser scanner is mounted to look downwards and the beam is scanned at right angles to the flight direction (see Figure 1<sup>1</sup>). Together with the forward motion of the aircraft, larger areas can be scanned. Even larger areas are measured by flying strip-wise above the terrain. This six degree of freedom trajectory defines a moving co-ordinate system for the observation

---

<sup>1</sup>Full color, high resolution versions of each figure can be found at <http://www2.wu.ac.at/alsopt>

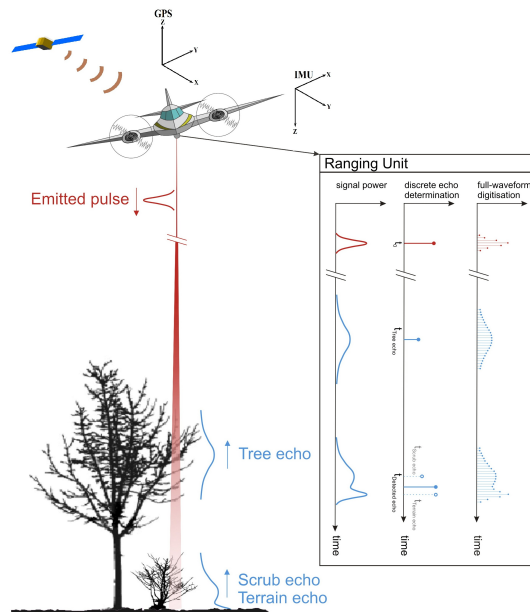


Figure 1: Diagram explaining the principles of ALS [3]

of range and angle from the laser scanner. With an Euclidean transformation the points can be transformed from the sensor co-ordinate system to the global co-ordinate system. Typical results for the accuracy of such points is in the order of 10cm (single standard deviation in each coordinate).

Besides the observation of distance between the sensor and an object point by the time lag of emission and detection of its echo, also other observations can be retrieved from the received echo. Firstly, it is not always the case that the laser beam hits exactly one object. Due to the diameter of the beam, e.g., 50cm, multiple objects may be within the beam, but at different heights. Examples include vegetation canopy and ground below. While a part of the signal is reflected at the leaves of the canopy of a tree, other parts of the signal continue traveling downwards until they hit lower vegetation or the ground, from which they are reflected. Thus, each emitted pulse may give rise to several echoes. Other examples, next to vegetation, are power lines and house edges, where a part of the signal is reflected on the roof, while the other part is reflected from the ground.

Furthermore, the backscattered echo can be sampled as a function of time, so-called waveform digitizing. The recorded amplitude depends on the range, on laser scanner device parameters, e.g. the receiving aperture diameter, but also on object properties, i.e., how much of the incident signal is absorbed, scattered diffusely, etc. By means of calibration [26] the parameters of the object like the backscatter cross-section, can be determined [27, 20]. The received echo may also be deformed relative to the emitted pulse. An increased echo width

[11] is a hint for either hitting a slanted surface or, more often the case, hitting vegetation. Within the footprint a number of leaves may be found which have similar by not identical height. Thus the echoes from all the leaves overlap and form a single widened echo.

## 2.2 Additional point descriptors

A point cloud  $\mathbf{P}$  is a collection of points  $p_i = (x, y, z) \in \mathbf{P}$  in a three dimensional space. The laser scanning point cloud can be analysed locally to enhance the description of each point further. For instance, given a point density of 4 points/m<sup>2</sup>, a local surface model [13] can be computed using e.g. the ten nearest points. This model may be an inclined plane, with it's normal vector being an additional description for the point. The equation of a plane through the point  $(x_0, y_0, z_0)$  having a normal vector  $n = (a, b, c)$  is given as

$$a(x - x_0) + b(y - y_0) + c(z - z_0) = 0 \quad (1)$$

To compute the three components  $(a, b, c)$  of the normal vector, three equations, i.e. three (non collinear) points are required. To add robustness, generally more than three points are used. A subset of points in the neighbourhood are typically selected based on  $k$ -nearest neighbours or points with in the sphere of a pre-defined radius. If  $k$  nearest neighbours are selected than there are  $k + 1$  points and subsequently  $k + 1$  equations (1). A least squares solution of this overdetermined system of equations estimates an optimal plane by minimizing squared sum of distances between the points and the estimated plane. In the matrix form this equation system is written as

$$A \cdot \beta = 0, \quad (2)$$

where each row of matrix  $A$  contains the coordinates of a point relative to the center  $[x_n - x_0, y_n - y_0, z_n - z_0]$ , here  $n = 1..k + 1$  and  $\beta = [a, b, c]^T$  is the unknown normal vector. The least squares solution for a system of equations of this (2) form is equivalent to solving the eigenvalue problem of the matrix  $A^T A$ . The unknown normal vector  $\beta$  of the estimated plane is the eigenvector corresponding to the smallest eigenvalue of  $A^T A$ . The matrix  $A^T A$  is often called structure tensor [7]. The mathematical form of the structure tensor is:

$$A^T A = T = \frac{1}{k} \sum_{i=1}^{k+1} (p_i - \bar{p})^T (p_i - \bar{p}) \quad (3)$$

here  $\bar{p} = (x_0, y_0, z_0)$  is the center of the points in the neighborhood.

For house roofs or street surfaces the normal vectors have been shown to reach an accuracy of a few degrees. The normal vector further allows to convert the backscatter cross section into the so-called diffuse reflectance. This value assumes a certain (Lambertian) scattering behavior of the object. This scattering mechanism is described by the reflectance (a unit-less value) and the normal

vector of the surface. A surface reflecting all incoming light perfectly diffuse has a reflectance of 1.

The quality of the plane fitting, e.g., the root mean square distances between the optimal plane and the given points indicates the roughness of the surface [10]. The smallest eigenvalue of  $T$  gives the variance of the distances between the points and the estimated plane.

The structure tensor  $T$  holds plenty more useful information about the distribution of points in the neighborhood. The geometric information encoded in  $T$  is essential in the characterization and classification of natural and artificial objects. Three widely used features derived from  $T$  are linearity, planarity and omnivariance. The linearity feature reflects how well the distribution of points can be modeled by a 3D line. Points over power lines exhibit such a characteristic, therefore, the linearity feature is essential in classifying power lines and similar structures. The planarity describes the smoothness of the surface which is directly related to the roughness measure and the quality of plane fitting for normal vector estimation. In contrast to power lines and smooth surfaces, laser echoes from trees often spread inhomogeneously across a larger 3D volume. This volumetric point distribution is described by the concept of omnivariance. These features are computed using the three eigen values  $\lambda_1 \geq \lambda_2 \geq \lambda_3 \geq 0$  of the matrix  $T$ :

$$L_T = \frac{\lambda_1 - \lambda_2}{\lambda_1} \quad (4)$$

$$P_T = \frac{\lambda_2 - \lambda_3}{\lambda_1} \quad (5)$$

$$O_T = \sqrt[3]{\lambda_1 \lambda_2 \lambda_3} \quad (6)$$

In addition to  $L_T$ ,  $P_T$  and  $O_T$ , features like anisotropy, eigenentropy and curvature are also derived using the eigenvalues of the structure tensor  $T$  [14, 8, 21, 28].

More information about the characteristics of the surfaces can be derived using features like *echo ratio*, *ZRange*, *ZRank*, *NormalizedZ* and *PointDistance*. *Echo ratio* represents the vertical penetration of the surface [9]. *ZRange* represents the maximum height difference between the points in the neighborhood, while *ZRank* is the rank of the point corresponding to its height in the neighborhood. *NormalizedZ* is the rank of the point (between 0 and 1) multiplied by the height range in the neighborhood. *PointDistance* is the average of all shortest distances between the points in the neighborhood. A more detailed description of these features can be found in [16, 19].

Thus, the point cloud can be augmented by additional parameters besides the coordinates  $x, y, z$ : the echo ID (first, second, . . . last echo of a sequence of echoes) and overall length of the echo sequence, echo amplitude, echo width, backscatter cross section, diffuse reflectance, roughness (*NormalSigma*), normal vector (*NormalX*, *NormalY*, *NormalZ*) echo ratio (*ER*), *ZRange*, *ZRank*, *NormalizedZ*, *PointDensity*, *PointDistance*, linearity, planarity, and omnivariance.

### 3 Classification

A major application for the automated processing of point clouds is the classification of points. In this application, every point is assigned a class due to its inherent laser return characteristics and its derived features. If successful, any such endeavor promises massive savings in terms of human resources and time, and thus ultimately in cost.

In the past, the remote sensing community focused on classifying data obtained from satellite measurements [15]. They report that results in general have been only somewhat satisfactory with large portions being continuously misclassified. In contrast we work with air- and not satellite-borne data. This allows for a much higher resolution and considerable less atmospheric interference when measuring. Further, the used full waveform data contains much more information than traditional approaches using laser solely for range measurements. Finally, the method of actively illuminating the ground with a laser beam is superior to passively recording reflections of sun light.

Classification tasks can be grouped into human and machine based classifications. Machine based classification itself can be split into knowledge- and learning based systems. The former is today's industry standard in ALS point cloud processing, the latter the eventual developmental goal. The main disadvantage of knowledge-based systems over machine learning classifiers is their requirement of explicit definitions of ontologies and classification rules. Machine learning classifiers, on the other hand base their classifications on rules automatically deduced from the available data with minimal (or no) human intervention. A machine learning classifier with human intervention uses initial human input to deduce automatically classification rules from it, that then can be used to autonomously classify points of previously unseen point clouds.

When charging humans with point classification, a number of factors come into play. Foremost, there is the need for additional data. Usually, this data is provided by means of orthophotos that are (ideally) taken in parallel to the laser scanning. Secondly, the qualification, endurance and accuracy of the employed human has to be taken into consideration as well. That person needs to be an expert user of geographical information systems and trained to recognize the subtleties of orthophotos.

This confluence of laser scanning data, external data via orthophotos and human experience allows for rather precise classifications of points. So far, human performance has not been surpassed by machines in terms of accuracy. Naturally, human classification is a very time consuming process. And equally naturally, machines outperform humans in the time domain by many orders of magnitude. Therefore, investigating algorithms for automated point cloud classification is an active area of research.

When turning to learning based classification, two approaches following the classical machine-learning dichotomy of supervised vs. unsupervised learning come to mind. The former requires initial human classifier input to derive a classification of unseen points, while the latter does not. The advantage of supervised classification is, that the resulting classes correspond with target

classes provided through human input. Since unsupervised classification lacks any human interaction, the classes found may or may not be interpretable or relateable to classes that humans would come up with. In the remainder of this section, we will focus on supervised classification based on initial human interaction and the difficulties that arise from it.

As detailed above and elsewhere [16], point characteristics can be grouped according to the way they were obtained: by direct measurement, by calibrated or spatial improved measurements, by deriving them computationally, by linking with meta data. For the former three groups, problems can arise. Directly measured point features are subject to the specifics of the laser scanner used. The predominant method employed for airborne laser scanning enterprises is a laser that is being deflected off the vertical by a rotating prism or a swinging mirror. This allows to scan a range perpendicular to the flight path and is essential for obtaining complete laser scans. However, this method changes the characteristics of the laser return signal, as the angle of the return signal not only depends on the characteristics of the surface, but also the angle of the inbound signal. For instance, when scanning directly below the aircraft only little occlusion will occur, while at extreme scan angles, the laser beam will be obscured by any objects between the aircraft and the ground. This distortion needs to be taken into consideration when working with point cloud data. Subsection 3.4 below discusses the detection of and compensation for these effects in greater detail.

A further question that needs addressing is rooted in the way derived attributes are being computed. Many such attributes are computed taking in account a neighborhood of points. Here, neighborhood size becomes a defining factor. Choosing an appropriate neighborhood size is far from trivial. However, neighborhood size theoretically affects the classification quality that can be derived. Further complications arise from different neighborhood sizes that can be chosen for each attribute. In subsection 3.5 we present a genetic algorithm for finding optimal neighborhood sizes for all neighborhood dependent features involved in the classification.

Before turning to the problems described above, we will briefly introduce the data set we worked with and describe how supervised classification works from human and machine perspectives, respectively.

### 3.1 Data set and example

From the industrial side of view, the motivation for this project was to find a new, fast and reliable algorithm for the classification of point clouds, which can minimize the manual checking and correction, because every manual manipulation is a very time consuming task. The scenario described in subsection 4.4 below was the basis for the development of the models used to automatically classify point clouds.

The data set used was taken from the project *DGM-W Niederrhein* with kind permission of the *Bundesanstalt für Gewässerkunde, Germany*. Four predefined areas have been selected, each not bigger than 60 hectares, with different content

like bridge, power lines, houses, coniferous and deciduous trees, concrete, gravel, bare earth, groynes and water.

The flight was done by airplane with the use of a Riegl LMS-Q560 200 KHz Laser Scanner. Flight speed was 100 knots at an altitude above ground of 600 meters. The distance between the flight lines was 300 meters. The effective scanning rate was set to 150 KHz with 80 lines per second. The resulting mean point density was about 6 points/m<sup>2</sup> over the whole area (except water areas). A radiometric calibration was computed using asphalt streets in each flight session as calibration reference. The calibration parameters were then applied to compute the reflectance, a normalized intensity value. Roughness shapes (derived from digital orthophotos), which define different ground classes of all areas were known and used as support.

For the classification a list of classes was discussed and defined. First a high-order list with standard classes (level 1), which are most common in the majority of laser scanning projects was generated; then each standard class was refined into subclasses (level 2) to better represent the different kinds of environment. The classes used for this project can be seen in Table 1.

Following the refined class list and taking the roughness shapes into consideration, a three dimensional classification was done manually using the TerraScan software package. This was done to provide reference data to generate training and testing data sets for the supervised classification method. Later the manual classification was also used as gold standard for assessing the results of the classification done with both the supervised and unsupervised methods.

### **3.2 Reference data generation through manual classification**

The term reference data refers to data that is manually classified by humans using external data sources like orthophotos. It serves two purposes: providing training data for supervised classification and representing a gold standard that can be used to test the automatic classification's accuracy.

One method to generate reference data is a manual classification of the data set [24, 12]. This process requires a thorough visual analysis of the data and a labeling of each point. As this process is time consuming, typically only small parts of the data set are manually labeled. Thus, this part should represent the diversity of the terrain surface (flat, hilly, etc.) as well as a large amount of the different target classes with a variety of geometric appearance and distribution of other measured or derived objects. These target classes often comprise natural objects (bare-earth, water, vegetation, etc.) and man-made objects (buildings, roads, bridges, ramps, power and other transmission lines, fences, cars and other moving objects, etc.). Vegetation, as one targeted class for example, can be tall and low and have different density. The variety of vegetation has to be included in the manually labeled part for both, accuracy assessment and machine learning. The diversity of classes depends on the purpose of the classification.

Reference data generation can be performed in a number of different ways. Firstly, an automatic classification based on a selection from available algorithms



Table 1: Defined classes in two levels of granularity.

<b>First level</b>		<b>Second level</b>	
Class	Code	Class	Code
unclassified	0	unclassified	0
undefined	1	undefined	1
ground	2	ground	2
		sand	18
		gravel	3
		stone, rock	4
		asphalt	22
		cement	21
		river dam, groyne	28
vegetation	5	deciduous forest	5
		coniferous forest	6
		mixed forest	7
building	8	building roof	8
		wall, building wall	24
water	9	water	9
artificial objects	10	car, other moving object	10
		temporary object (under construction)	11
		bridge	12
		power line	13
		tower, power pole	14
		bridge cable	15
		road protection fence	16
bridge construction	17		
technical	23	technical, e.g. concrete part of a bridge	23
ground, vegetation	20	ground, vegetation	20
error	99	error	99

can be performed, followed by a manual improvement of the results. Secondly, only manual classification of an unclassified data set can be performed. In the case of a large number of classes the second way is recommended. A third option in the generation of reference data by using existing data sets. As those data sets were often acquired at a different time, with a different measurement technology, and often with other applications in mind, the transferability of such a classification is limited. Therefore, the next paragraphs will concentrate on the methods for manual classification.

The most common methods for visualization and reference data generation are described below. The basic and most common method uses a 2D profile (Figure 2). Profiles are sets of points cut out from the entire point cloud with a vertical rectangular prism, not bound in height. The width of the prism is typically small, e.g. 2 m, whereas its length is larger, e.g. 50 m. These values are sensible when working with point densities ranging from 1 to 20 points/m<sup>2</sup>. Profiles allow the user to see a part of the terrain from a side view which enables her to distinguish the points within different classes but also to identify the border between different objects, e.g. building and ground, or vegetation and ground. These borders are harder to identify in a top view. In order to classify larger areas in an organized manner, transects are used. This means that a set of parallel profiles is generated which cover a rectangular area. Advancing in the manual classification from one profile to the next accelerates the entire process. The second method uses a shaded relief map (hillshade) of the surface generated by the points of one class. A hillshade requires an artificial illumination source, which is set in a standard manner to an azimuth of 315 degrees, lighting the area from the northwest. Lighting from different directions can substantially help to notice the terrain slope as well as objects located on the ground, especially in the case of mountainous regions. Hillshades can be generated for the bare-earth class, in which the surface represents the digital terrain model (DTM). An example for transects and hillshades can be found in the top panel of Figure 2. That figure's bottom panel exhibits a DTM. Also combinations of classes, e.g. bare-earth and buildings, can be used. This method can be applied for refining a manual classification, i.e. reclassifying points. This is especially suited to remove small artifacts which occur when close spatial proximity between two classes led to a misclassification in an earlier step.

### 3.3 Supervised classification

The idea behind supervised classification is to automatically derive from a small training set enough classification rules, so that a larger, unseen data set can be classified automatically using the model derived from the former. For that purpose, the training data needs to be classified already. Usually, this initial classification is achieved by manually classifying the points. This training data is then used to build a model or equally train the classifying algorithm. In supervised classification, the interpretation of the model comes second, therefore more complex models are favored over simplistic ones that would ease human interpretation; in fact, the boundary to model complexity is dictated only by

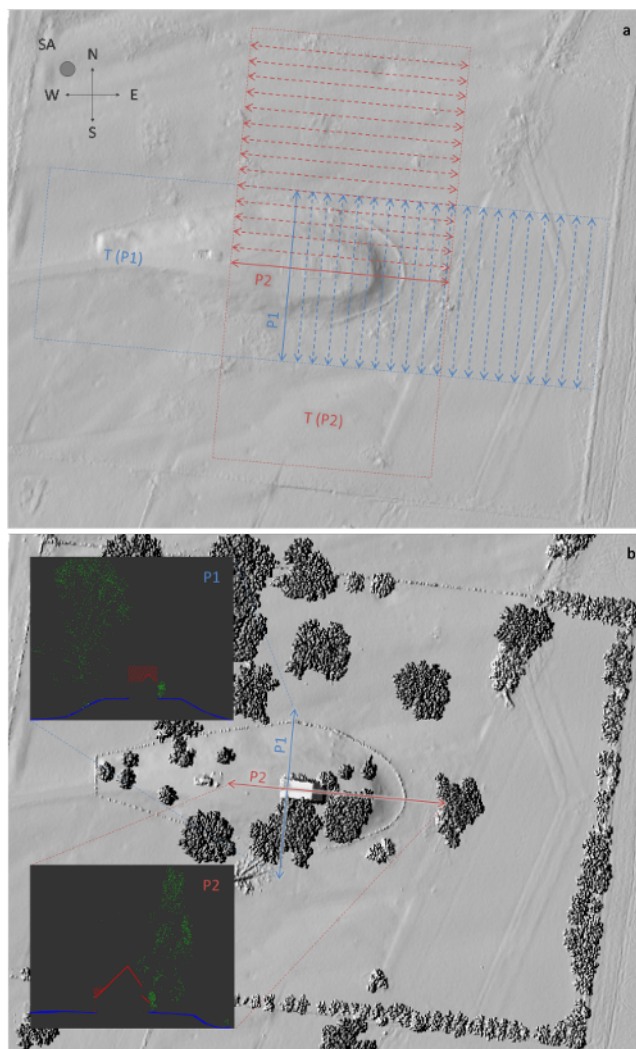


Figure 2: Methods for visualizing the data during manual classification; a – shaded relief for DTM; b – shaded relief for DTM, buildings and vegetation; P1, P2 – 2D profiles; T(P1), T(P2) – transects for 2D profiles; SA – sun azimuth for shaded relief

overfitting avoidance. This model is then used to classify unseen data. To evaluate model performance, true classification information for the unseen data is required as well. However, in production environments, model evaluation for the entire data set is usually not performed. Therefore, supervised classification promises to save a considerable amount of costs.

The method of choice for supervised classification here is classification trees. The tree is a predictive model that links up point features with that point’s class. Structurally, the tree consists of leaves and branches. The leaves represent the final class labels and the branches the conjunctions of features that lead up to these class labels. Literature suggests a number of different algorithms for growing a tree [23, 15]. For the purpose of classifying point clouds, we have found Breiman et al’s Classification and Regression Trees (CART) [1] to strike a good balance between computational complexity and reliability. The implementation we used was that of rpart [25]. In terms of Friedl et al. [5] these trees are univariate classification trees.

Conceptually, a classification tree seeks to partition the entire feature space of a data set, one variable at a time. It does that by selecting a variable and an appropriate splitting value that will contribute maximally to node purity. Node purity is computed using the Gini impurity coefficient:

$$I_G(f) = 1 - \sum_{i=1}^m f_i^2 \quad (7)$$

with  $f_i$  being the fraction of items labeled to be of class  $i$  for a set of  $m$  class labels.

This splitting and branch growing continues, until no variable can be found that further increases node purity. The resulting trees can become quite large which hinders interpretation (not a problem for point cloud classification) and are prone to overfitting. This latter limitation can become troublesome when trying to classify point clouds, as the learned model does not generalize well anymore for unseen data. However, using cross-validation and pruning off branches that are not occurring in a significant number of replications, proves to be an effective tool against overfitting.

As stated above, the performance of a classification tree can be gauged if not only training but also test data contain true class labels. A measurement statistic of classification performance is the misclassification rate. Let  $M$  be a cross-classification matrix between true and predicted class labels and its elements being the counts of the predicted elements and  $J$  the number of all points in the point cloud, then

$$MCR = 1 - tr(M)/J \quad (8)$$

is the misclassification rate.

When selecting training data, two factors need consideration: the randomness of the selection process and its stratification. The former factor becomes important once large sets of random numbers need to be created. While computers can always only generate pseudo random numbers, most of them are

sufficiently strong for point cloud processing.<sup>2</sup> However, strong random number generation with guaranteed randomness does not suffice to select a suitable training data set, if the classes are not evenly distributed. In that common case, single classes—say temporary construction structures—have only very few points associated with them. When choosing points at random, it is extremely unlikely that many of the rare class points will end up in the training data set. And if a class does not show up in the training data set, the supervised classification algorithm cannot learn the rules required to classify it. Therefore simple random sampling schemes do not work in the presence of rare classes.

To enable the supervised classification of rare classes, stratified sampling needs to be applied. In its simplest form, stratified sampling guarantees that numerous points from each class are selected for the training data set. This, at the expense of having the entire training data set being representative for the point cloud it has been sampled from. The heuristic used for our stratified sampling approach sets the size of the sample for stratum  $c$  ( $s_c$ ) to be either half of the points of that class ( $S_c$ ) or the overall sample size ( $k$ ) divided by the number of classes in the point cloud ( $|A|$ ):

$$s_c = \min\left(\frac{S_c}{2}, \frac{k}{|A|}\right) \quad (9)$$

As noted above, the resulting stratified sample is not representative for the entire point cloud anymore: rare classes occur much more often in the training data set than they do in the point cloud. It is therefore necessary to inform the supervised classification algorithm of that misrepresentation.

Perhaps obviously, the performance of a tree depends on the number of data points it is allowed to learn from: the larger the training data set, the better (usually) the classification of test data will be. However, manually classifying points is expensive. Therefore, it is crucial to find a training data set size that is just large enough to produce reliable predictions. Figure 3 depicts this relationship. As can be seen, there is a sharp drop between 10,000 and 20,000 points as training data set size with respect to mean misclassification rate and its dispersion. After about 50,000 points, the improvement gained by adding additional points subsides. We therefore settled for 50,000 points as training data set size. The resulting mean misclassification rate of 0.065 is a usable starting point. In the following, we will discuss aspects of improving this achievement even further.

When classifying point cloud data into predetermined classes, not all classes that appear to be epistemologically justified to humans can be sufficiently identified using laser return signals. For the problem at hand, the points were to be partitioned into 26 classes. Logically, these classes could be broken down into coarsely and finely grained classes. While the coarse classes were successfully classified (MCR: 0.02,  $\sigma = 0.002$ ), the finer classification exhibited the 6.5% MCR as described above. Table 2 lists the finely grained classes that were no-

---

<sup>2</sup>We used the R [18] implementation of the Mersenne twister, which has a period of  $2^{19937} - 1$ .

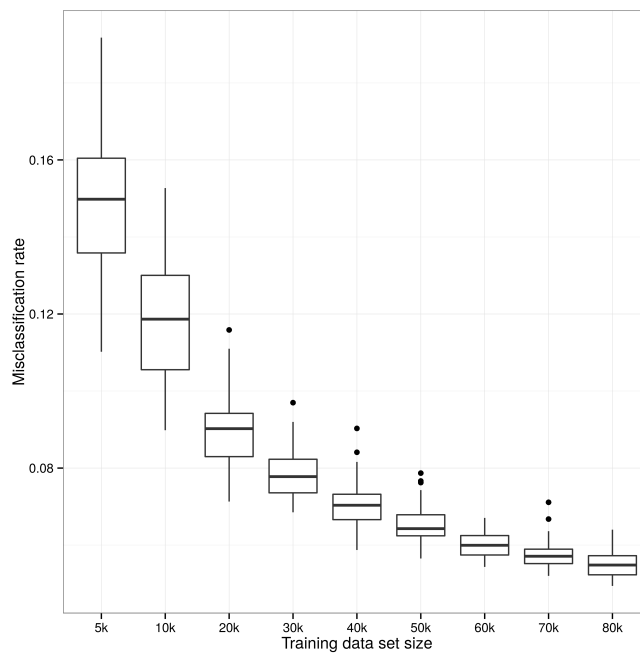


Figure 3: Misclassification rate as a function of training data size; classification of a 3 million strong point cloud, results bootstrapped with 50 replications

Table 2: Classes that were hard to predict. Percentage of points that ended up in that class. Remainder to 100 percent is scatter in all classes.

True class	Predicted classes
Building, wall	Deciduous forest (67%)
	Building roof (17%)
	Building, wall (17%)
Temporary object	Temporary object (78%)
	Road protection fence (14%)
Power pole	Power pole (75%)
	Road protection fence (16%)
Error class points	Scattered in all classes

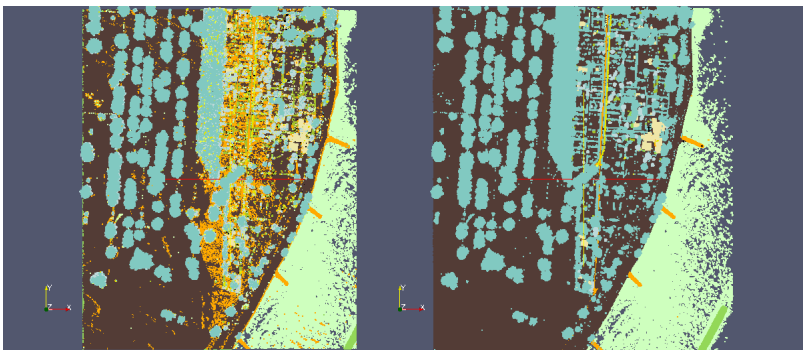


Figure 4: Predicted (left) and true (right) classification of a sample area

toriously troublesome. Figure 4 shows the differences between automatic and true human classification results.

When casting a more detailed look at these misclassifications, it becomes evident that many of them are conceivably caused by imprecise classifications of humans in the first place. Consider for example a road in winter: the asphalt tarmac is at places covered with grit sand to prevent the icing of the road. Grit and asphalt tarmac will differ in texture and material. Therefore, the laser return signal for patches of road that contain more grit sand than others will exhibit different characteristics. In manual classification based on aerial photography, these patches of grit sand are unlikely to be identified and marked as such by the human classifier. To a certain extent, the misclassification rate achieved by supervised classification of finely grained classes can be explained by the algorithm outperforming human classification. This is obviously very dependent on the quality of human classification.

A similar argument holds for the error class. Here, points were classified as errors if some of their measurements exceeded a valid measurement range. The

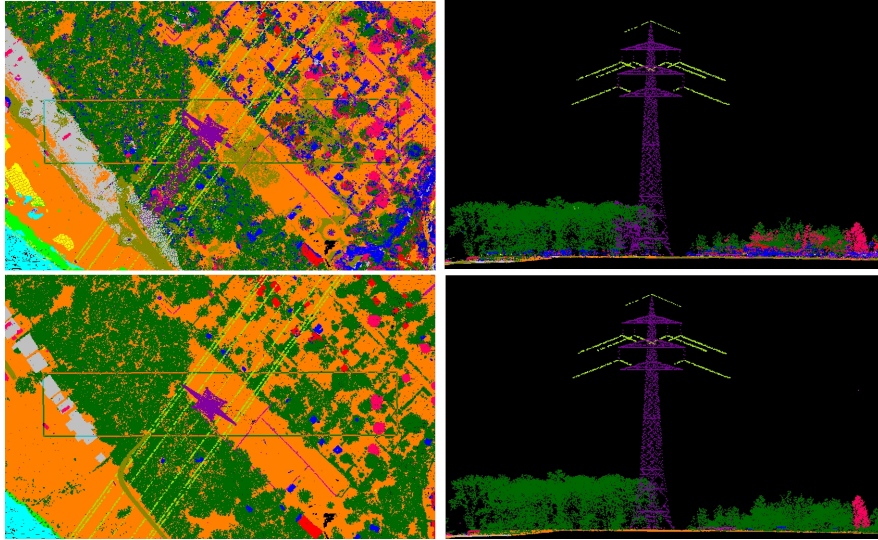


Figure 5: Misclassification at a power line where pole and vegetation cannot be separated reliably; automatically classified point cloud on top, bottom panel shows the manually classified one

algorithm was informed about these missing values. On the other hand, classification trees are able to cope with missing information by substituting it with the second best split. Therefore, points that a human would not classify because it contained obviously faulty measurements, were classified by the algorithm.

Another problem that is rooted in the difficulty of epistemological concepts is the misclassification of many temporary object points as road protection fences. It is difficult for any automated classifier to learn the concept of an object being temporary in nature. While the algorithm successfully classifies almost all temporary objects as some kind of artificial objects, it cannot differentiate between these objects being permanent or temporary (road protection fences).

However, the largest problem in misclassification cannot possibly be rooted in epistemological complexities: Buildings and walls are being classified predominantly as trees. From a geometrical point of view, trees and buildings do indeed share some properties related to their height and volume. On the other hand, distinctive characteristics like texture and material should have been picked up by the algorithm. This type of mistake is also represented in Figure 5. To some extent, the misclassifications can be explained by snow or leaf covered roofs on top of buildings. Still, this unsatisfactory performance can most likely only be overcome by implementing geometrical shape detection in a post-processing step. This is the focus of ongoing research.



Table 3: Model quality in mean MCR for models with different kinds of border effect components. Results bootstrapped with 50 replications.

<b>Model type</b>	$\mu_{MCR}$	$\sigma_{MCR}$
no border effects	0.081	0.004
beam vector components	0.065	0.005
scan angle	0.074	0.005
beam vector components and scan angle	0.063	0.004

### 3.4 Border effects

Airborne laser scanning is limited by the principles of optics: dependent on the incident angle, the characteristics of a laser return signal varies. For example, hitting vegetation from the side will produce many more laser echoes than hitting it straight from above. Also, the shape of the beam’s cross section depends on that angle. Additional distortion in the characteristics of points may arise from the method of aerial laser scanning. Due to the limited field of view of airborne laser scanners wider areas are scanned by multiple overlapping strips. Typically, these strips overlap to achieve full coverage even in case of wind sheer or minor navigation errors. In these overlapping areas, the properties of the measurement process change (as there are multiple overpasses); a change that needs to be accounted for.

One method to compensate for the different return signal quality/properties is to take the deflection of the laser into account. There are two approaches available. One uses the raw beam vector components ( $v_x, v_y, v_z$ ) that indicate the deflection of the laser beam for a given point. The other method combines these components to derive the scan angle  $\phi$ :

$$\phi = \arctan\left(\frac{\sqrt{v_x^2 + v_y^2}}{|v_z|}\right)$$

The following Table 3 shows the effect beam vector components and scan angle have on the misclassification rate. Starting with the simplest model without any compensation for border effects, the mean classification rate lies at 8.1%. Adding the scan angle to the model improves its quality by one, beam vector components by two percentage points. Adding both compensation terms to the model barely improves classification quality with respect to a pure beam vector components model.

### 3.5 Scale space selection

A number of point cloud features are not directly measured but computed with respect to any points immediate neighborhood. In general, the local neighborhood of a point can be defined in 2D or 3D. Furthermore, a certain number

Table 4: Parameters of the genetic algorithm.

<b>Parameter</b>	<b>Value</b>
Population size	100
Tournament size	5
Mutation probability	0.05
Elite proportion	0.1
Reseed proportion	0.1

of closest neighbors, a fixed distance or a combination of both can be used as neighborhood definition. For the following analysis a cylinder (i.e. 2D fixed distance neighborhood) for each point is formed. Obviously, larger radii lead to a stronger averaging effect while smaller ones are prone to overfitting. It, therefore, is important to find the optimal radius for each feature in order to minimize misclassification rate.

To discover the optimal radii for neighborhood-dependent features, a genetic search algorithm [6] was used. In the following we will describe the genetic algorithm used for this optimization and its parameters. We then turn our attention towards evaluating the algorithm’s performance in terms of convergence and solution stability. The former examines the relation of improvement achieved due to and time spent on optimization. The latter analyzes the stability of recommended radii across a number of optimizations.

The 13 neighborhood-dependent features were computed each with radii ranging from 1 to 6 m in 0.5 m increments resulting in 11 versions of each feature. The algorithm’s genomes were then modeled to be integer vectors of length 13 with each gene being an integer from 1 to 11, encoding the chosen neighborhood size for each feature. The algorithm was initialized with 100 random genomes as starting solutions. The standard genetic operators of single-point cross-over breeding and mutation were employed for evolutionary optimization. Further, pairing genomes for mating was done using tournament selection and a proportion of the top performing solutions was cloned directly into each new generation. To ensure that the gene pool remained fresh and to safeguard against local optima traps, some random genomes were introduced with each generation. Table 4 gives the parameters of the genetic algorithm, which were established by experiment.

The fitness function to be optimized was the misclassification rate as described above. In order to ensure comparability, MCR was computed using the same training–test data split each time. The initial split was generated using a stratified sampling scheme and included 5137 points in the training data set. Using a random sample of 100,000 points, the algorithm was allowed 500 generations to find the optimum combination of radii for the 13 neighborhood-dependent features. In order to ensure computability within reasonable time, not the entire point cloud could be processed. Therefore, a very large simple random sample of 100,000 points was drawn from the point cloud, and all

operations were performed on that sample.

As genetic optimization is essentially stochastic in nature, the optimization was repeated 34 times. Of these 34 replications, 30 reached the same optimum while 4 stayed behind (by a very small margin). Almost all replications had converged to the optimum after 50 generations. By generation 75 all 30 successful replications had converged. The optimum discovered implied a misclassification rate of 0.022. When compared to the best misclassification achieved using a constant radius of 6 meters (0.065) this is a notable improvement by more than 60 percent.

Turning to solution stability, it is of interest whether each replication's terminal solution leads to the same combination of radii or not. Figure 6 displays a heat map of cylinder radii per feature chosen in each (optimal) replication. Features that exhibit the same color shades for the entire column can be considered stable. These are the variables NormalizedZ, NormalZ and PointDensity. For each of these features, the optimal cylinder radius is at 1 meter. At the other end of the spectrum, very colorful columns, Linearity, Planarity and Z-Range, are indicative of features whose neighborhood size has no impact on misclassification rate.

The genetic algorithm delivers a definite improvement of the misclassification rate. The remaining two percent are most likely due to measurement and human classification error. With respect to solution stability, it became obvious that while some features are computationally dependent on neighborhood size, the outcome is not affected by them. On the other hand, there are features that clearly exhibit a strong dependence on neighborhood size. Conceptually, the genetic algorithm can be improved by implementing consensus voting when delivering radii recommendations. This too, is an ongoing research effort.

We conclude that supervised classification of point clouds is definitely an idea worthwhile pursuing. The data quality obtained from airborne laser scanning allows for a very precise analysis of the ground. In combination with the sophisticated computation of derived point cloud features, advanced classification algorithms sampling schemes as well as evolutionary optimization strategies, we are able to produce classification accuracies that surpass classical satellite based classification. While the classical approaches rarely ever reach above 90 percent accuracy, our approach delivers consistently accuracies close to 100 percent. While there are challenges that remain to be overcome, the achieved accuracy is already good enough for many applications. In the following we will discuss these applications further.

## 4 Industrial applications

Airborne Laser Scanning is in use for industrial purposes since the mid 1990s and has dramatically improved since then. For example: in the beginning there have been laser scanners with a fixed array of fibre optical conductors, which brought a good point density in the direction of flight, but very poor density in the transverse direction. So a detection of embankments along the

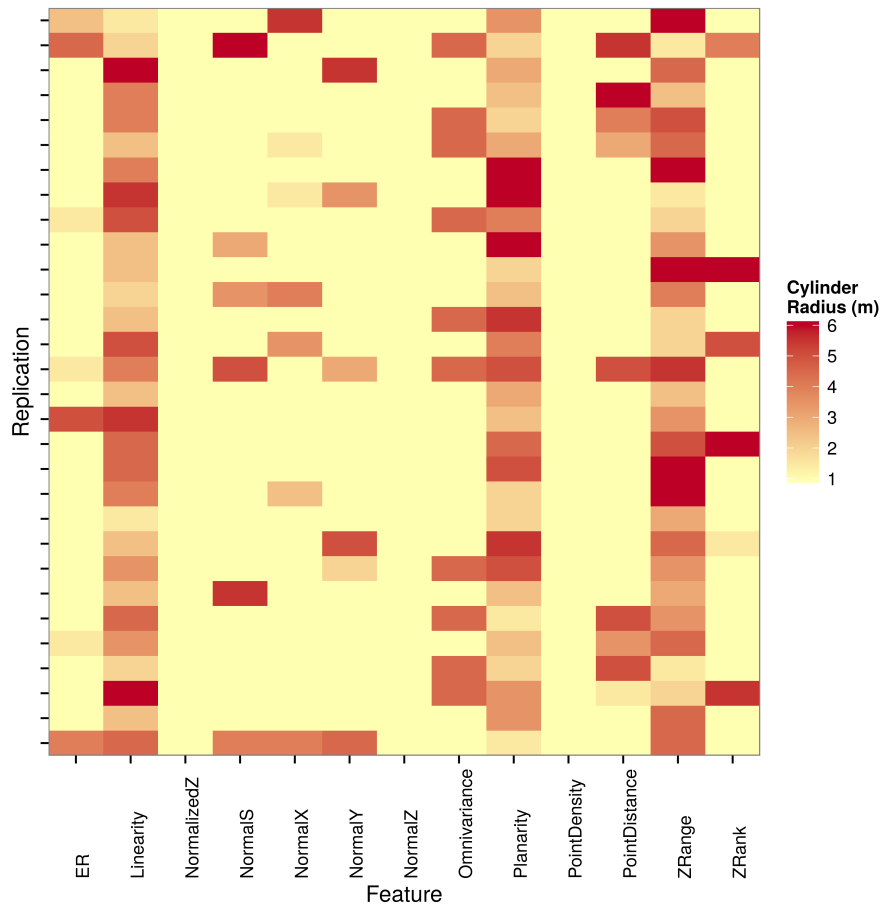


Figure 6: Solution stability of 30 genetic optimization replications

flight direction was very hard. Technological advances like the steadily increased measurement rates, improved apertures and new detection algorithms prepared the way for a wide field of applications.

There are different technologies at work in today's laser scanners: they provide sampling rates of up to 600,000 laser pulses per second. Also modern apertures are able to detect more than just one single return per pulse and provide reflectance, echo ID and echo width for each return; some can even penetrate water surfaces and give information on submarine ground and submerged objects.

Higher point densities result in better environment depicting. With today's high point densities, embankments can be well detected by extracting *breaklines* within the point clouds. Normally 4 points/ $m^2$  will be ordered, but customers more often want 8 or more points/ $m^2$ . This gives the opportunity to model the ground more precisely. But customers are not only interested in the presence of ground, they also want to know what kind of ground they are looking at.

Classification is mostly a semiautomatic process, consisting of an automatic step and a manual checking and correction step. One of the aims is to minimize the need of manual correction, due to its cost. Another aim is to improve the automatic detection of more than a standard set of classes to cater to future customer's requirements.

In the following we will present some examples of airborne laser scanning applications.

## 4.1 Digital Terrain Model

Often a plain model of the ground is needed for planning or research purposes. These models are of great importance for e.g. road- or railway planning offices, to know how much material has to be removed or added for street or railway planning. Therefore the point cloud has to be classified with special emphasis on detecting erroneous echoes. The DTM classes mostly consist of ground, water and unclassified points, which have no influence on the model.

## 4.2 Digital Surface Model

The DSM features ground, vegetation, buildings, bridges and sometimes power lines and describes the earth's surface including natural and artificial objects. By subtracting the DTM from the DSM the result will be a normalized DSM. This can then be used for e.g. easy measurement of building or vegetation heights.

## 4.3 Avalanche prediction

In mountainous areas avalanches (snow or boulders) are a common threat, so prediction and subsequently protection is an important task. For aviation purposes it is also necessary to know the position of power lines or cable-cars. Therefore each point needs to be classified along the lines of ground, various vegetation, water, building, power lines, ...

To compute the pathways and probabilities of avalanches in certain areas, one not only needs to know point classes, but also inclination, roughness (in this case roughness refers to a parameter, which will tell how fluids will be slowed on a surface), azimuth, ...

All these features can be derived out of the point cloud by classifying using the above algorithm.

#### 4.4 Flooding prediction

To protect people and environment in areas that are in danger of flooding around rivers, it is vital to know, how water is flowing over different types of ground. Therefore ground has to be classified in different roughness classes, that have known properties for flowing or seeping. The classification of roughness areas is normally done by digitizing digital orthophotos [17, 4]. In respect to the classification methods described in section 3, roughness can be set in direct relation with different ground classes. Taking into account the derived DTM together with the digitized breaklines [2], a triangulated surface can be computed.

By combining the DTM surface with information of the different point classes from ground detection, there can be defined areas with varying roughness. This classification is normally done by using digital orthophotos as reference. By classifying the roughness purely from the data contained within a laser point cloud, the high cost of extra orthophotos can be skipped.

#### 4.5 Forestry and Vegetation

The detection of forested areas is an important part of environmental applications. Especially time series analyses, e.g. to estimate deforestation, was often carried out using analog or digital orthophotos so far. However, Airborne Laser Scanning gets more popular for such applications, because it is not restricted to the canopy. The laser beam can often penetrate the vegetation returning multiple echoes. This provides information about the vertical structure of the forest including good knowledge of the ground, which is needed to compute high quality DTMs, tree heights, stem volumes, etc. In urban areas the knowledge of classified vegetation is used in applications for 3D visualizations, urban planning, noise emission charts, etc. [22].

### 5 Conclusion

In this chapter we presented an overview of advances in processing and automatically classifying point clouds from airborne laser scanning. Particularly, the accuracy of the classification of point clouds can be improved greatly using machine learning based methods like decision trees. There, manually classified training data—a small subset of the entire point cloud—is used to build a classification model. This then in turn can be used to classify the remainder of the point cloud or a fresh one.

These advances in classification accuracy are chiefly due to our making use of the entire full wave form of the laser echoes. Using advanced radiometric and computational methods, for every echo additional properties or features are computed from that echo's wave form, external data and the echo's immediate neighborhood. Using an evolutionary algorithm we were able to identify features where the size of that neighborhood influenced classification accuracy and establish optimal neighborhood size values for these features.

The model presented in this chapter has applications ranging from forestry to avalanche and flooding protection. A more immediate application is the automatic generation of maps. However, this is but the beginning of our journey. We already pointed to the inclusion of shape detection for improving classification accuracy and consensus voting the genetic algorithm to optimize neighborhood size recommendations as current research goals. Further extensions focus on better understanding how the scan angle affects echo properties when analyzing the flights strip-wise. A major issue is the possibility to learn from multiple but possibly unreliable sources. Often, orthophotos related to a point cloud are out-of-date or older maps are used to provide external reference data. Ideally, if we were able to use these data sources to speed up training data and model generation, the entire remote sensing work flow could be revolutionized.

## References

- [1] Breiman, L., Friedman, J., Olshen, R., Stone, C.: Classification and Regression Trees. Monterey, CA (1984)
- [2] Briese, C., Mandlbürger, G., Ressler, C., Brockman, H.: Automatic break line determination for the generation of a DTM along the river Main. In: ISPRS Workshop Laserscanning 2009, pp. 236–241 (2009)
- [3] Doneus, M., Briese, C., Fera, M., Janner, M.: Archaeological prospection of forested areas using full-waveform airborne laser scanning. *Journal of Archaeological Science* **35**(4), 882 – 893 (2008)
- [4] Dorninger, P.: Eine praktikable und genaue Methode zur Bestimmung von Wasser-Land-Grenzen aus Laser-Scanner-Daten. *BfG-Veranstaltungen* **3**, 93–100 (2011)
- [5] Friedl, M., Brodley, C.: Decision tree classification of land cover from remotely sensed data. *Remote Sensing of Environment* **61**(3), 399–409 (1997)
- [6] Goldberg, D., Holland, J.: Genetic algorithms and machine learning. *Machine Learning* **3**(2), 95–99 (1988)
- [7] Gressin, A., Mallet, C., David, N.: Improving 3D LiDAR point cloud registration using optimal neighborhood knowledge. *ISPRS Annals of Photogrammetry, Remote Sensing and Spatial Information Sciences I-3* pp. 111–116 (2012)

- [8] Gross, H., Thoennesen, U.: Extraction of lines from laser point clouds. In: Symposium of ISPRS Commission III: Photogrammetric Computer Vision PCV06. International Archives of Photogrammetry, Remote Sensing and Spatial Information Sciences, vol. 36, pp. 86–91 (2006)
- [9] Höfle, B., Hollaus, M., Hagenauer, J.: Urban vegetation detection using radiometrically calibrated small-footprint full-waveform airborne LiDAR data. *ISPRS Journal of Photogrammetry and Remote Sensing* **67**(1), 134–147 (2012)
- [10] Hollaus, M., Aubrecht, C., Höfle, B., Steinnocher, K., Wagner, W.: Roughness mapping on various vertical scales based on full-waveform airborne laser scanning data. *Remote Sensing* **3**(3), 503–523 (2011)
- [11] Höfle, B., Hollaus, M., Lehner, H., Pfeifer, N., Wagner, W.: Area-based parameterization of forest structure using full-waveform airborne laser scanning data. In: *Silvilaser 2008*, p. 9. Edinburgh, Scotland (2008)
- [12] Kobler, A., Pfeifer, N., Orginc, P., Todorovski, L., Oštir, K., Džeroski, S.: Repetitive interpolation: A robust algorithm for DTM generation from aerial laser scanner data in forested terrain. *Remote Sensing of Environment* **108**(1), 9–23 (2007)
- [13] Kraus, K., Pfeifer, N.: Advanced DTM generation from LiDAR data. In: *International Archives of the Photogrammetry, Remote Sensing and Spatial Information Sciences*, pp. 23–30. Annapolis, MD, USA (2001)
- [14] Mallet, C., Bretar, F., Soergel, U.: Analysis of full-waveform LiDAR data for classification of urban areas. *Photogrammetrie Fernerkundung Geoinformation* **5**, 337–349 (2008)
- [15] Mather, P., Tso, B.: *Classification Methods for Remotely Sensed Data*. CRC press (2010)
- [16] Otepka, J., Ghuffar, S., Waldhauser, C., Hochreiter, R., Pfeifer, N.: Geo-referenced point clouds: Data model, features and management. *ISPRS International Journal of Geo-Information* **2**(4), 1038–1065 (2013)
- [17] Prinz, R.: DGM-W-Modellierung unter Einbeziehung erfasster Bühnen und Bühnenfelder. *BfG-Veranstaltungen* **3**, 48–57 (2011)
- [18] R Core Team: *R: A Language and Environment for Statistical Computing*. R Foundation for Statistical Computing, Vienna, Austria (2013)
- [19] Research Groups Photogrammetry and Remote Sensing: *OPALS: Orientation and Processing of Airborne Laser Scanning data*. Department of Geodesy and Geoinformation, TU Vienna, Vienna, Austria (2013)



- [20] Roncat, A., Bergauer, G., Pfeifer, N.: B-spline deconvolution for differential target cross-section determination in full-waveform laser scanning data. *ISPRS Journal of Photogrammetry and Remote Sensing* **66**(4), 418–428 (2011)
- [21] Rusu, R.: Semantic 3D object maps for everyday manipulation in human living environments. Ph.D. thesis, München, Techn. Univ., Diss., 2009 (2009)
- [22] Rutzinger, M., Höfle, B., Pfeifer, N.: Detection of high urban vegetation with airborne laser scanning data (2007). *Proceedings of ForestSat 2007*
- [23] Safavian, S., Landgrebe, D.: A survey of decision tree classifier methodology. *IEEE Transactions on Systems, Man and Cybernetics* **21**(3), 660–674 (1991)
- [24] Sithole, G., Vosselman, G.: Experimental comparison of filter algorithms for bare-earth extraction from airborne laser scanning point clouds. *ISPRS Journal of Photogrammetry and Remote Sensing* **59**(1–2), 85–101 (2004)
- [25] Therneau, T., Atkinson, B., Ripley, B.: `rpart`: Recursive Partitioning (2013). R package version 4.1-3
- [26] Wagner, W.: Radiometric calibration of small-footprint full-waveform airborne laser scanner measurements: Basic physical concepts. *ISPRS Journal of Photogrammetry and Remote Sensing* **65**(6), 505–513 (2010). *ISPRS Centenary Celebration Issue*
- [27] Wagner, W., Ullrich, A., Ducic, V., Melzer, T., Studnicka, N.: Gaussian decomposition and calibration of a novel small-footprint full-waveform digitising airborne laser scanner. *ISPRS Journal of Photogrammetry and Remote Sensing* **60**(2), 100–112 (2006)
- [28] Weinmann, M., Jutzi, B., Mallet, C.: Feature relevance assessment for the semantic interpretation of 3D point cloud data. *ISPRS Annals of the Photogrammetry, Remote Sensing and Spatial Information Sciences II-5/W2* pp. 313–318 (2013)